

## Supporting Information

### Chiral Mononuclear Lanthanide Complexes and the Field-induced Single-ion Magnet Behaviour of Dy Analogue

Shuang-Yan Lin,<sup>a, b</sup> Chao Wang,<sup>a</sup> Lang Zhao,<sup>a</sup> Jianfeng Wu,<sup>a, b</sup> and Jinkui Tang<sup>\*a</sup>

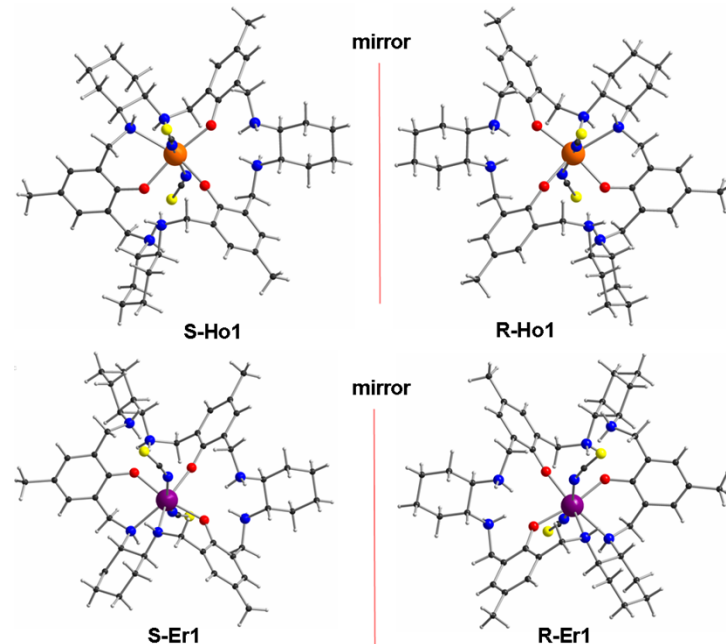
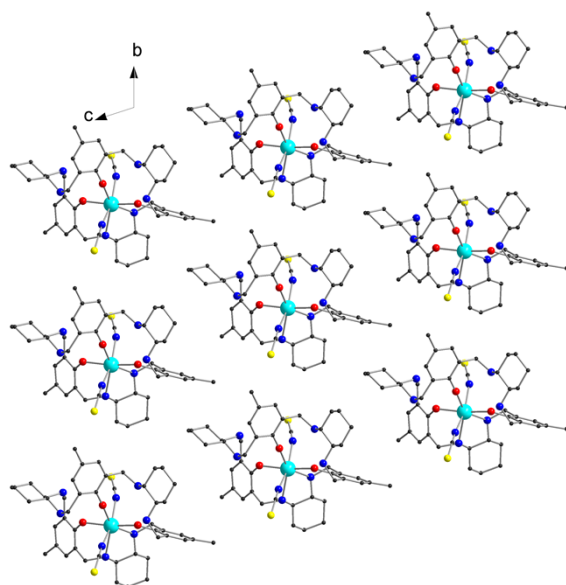


Fig. S1 Top: Enantiomeric pair of **S-Ho<sub>1</sub>** and **R-Ho<sub>1</sub>**; Bottom: Enantiomeric pair of **S-Er<sub>1</sub>** and **R-Er<sub>1</sub>**.



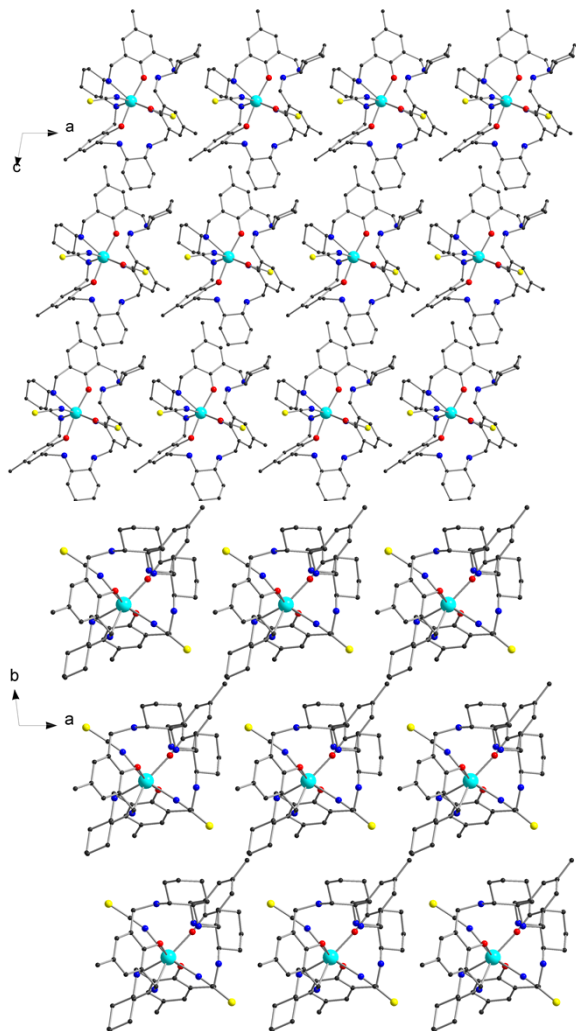


Fig. S2 Crystal packing of compound R-Dy<sub>1</sub> along the crystallographic *a*, *b* and *c* axis, repectively, showing a line arrangement along crystalline axis.

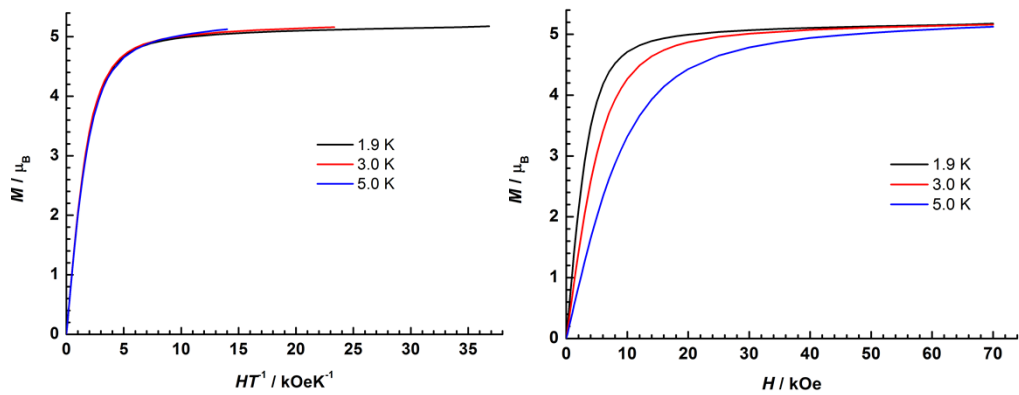


Fig. S3  $M$  vs.  $H/T$  plots and  $M$  vs.  $H$  plots at different temperatures below 5 K for **R-Dy<sub>1</sub>**.

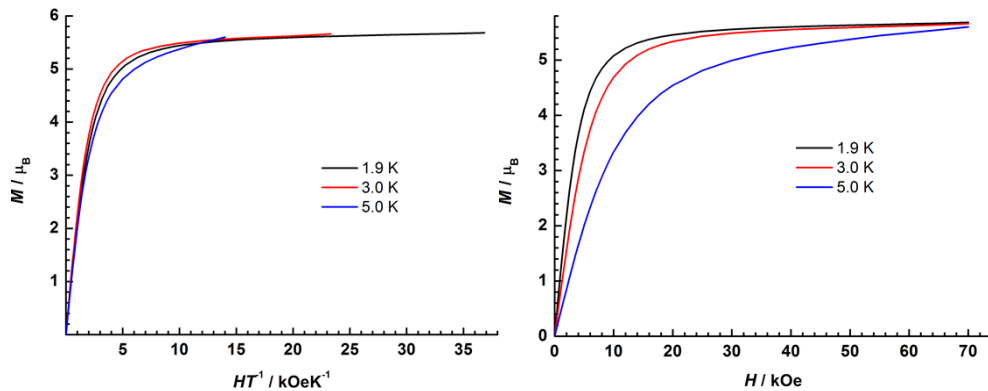


Fig. S4  $M$  vs.  $H/T$  plots and  $M$  vs.  $H$  plots at different temperatures below 5 K for **R-Ho<sub>1</sub>**.

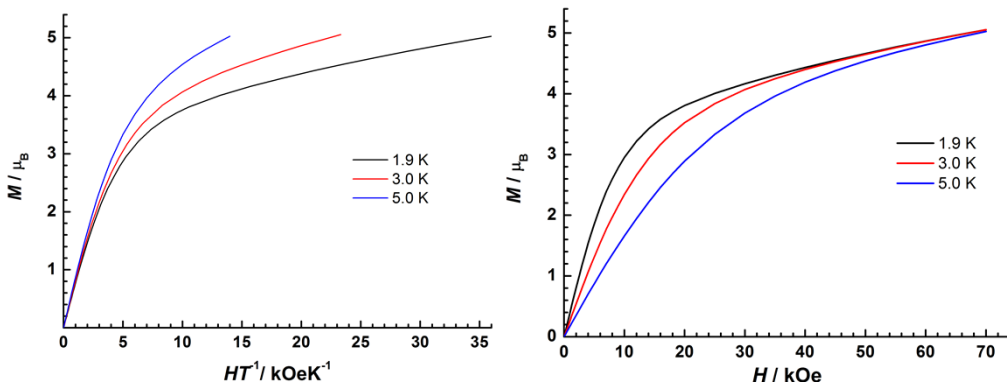
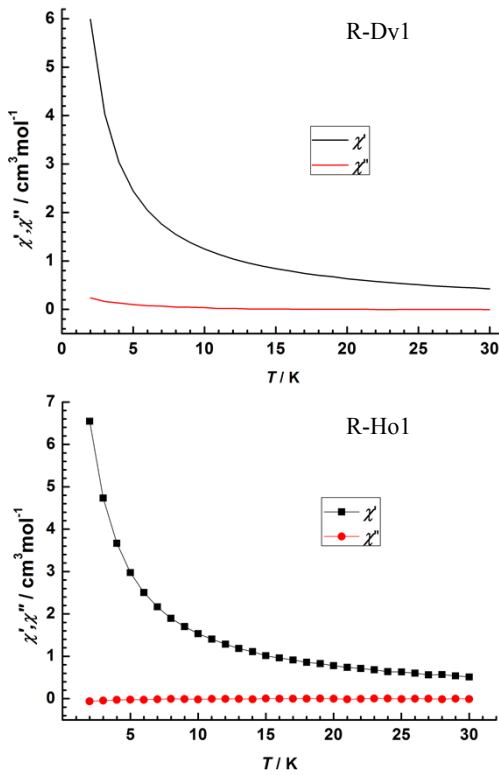


Fig. S5  $M$  vs.  $H/T$  plots and  $M$  vs.  $H$  plots at different temperatures below 5 K for **R-Dy<sub>1</sub>**.



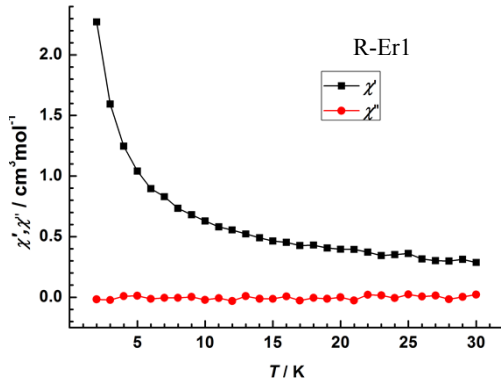


Fig. S6 Temperature dependences of  $\chi'$  and  $\chi''$  measured at 1000 Hz under zero dc field for **R-Dy<sub>1</sub>**, **R-Ho<sub>1</sub>** and **R-Er<sub>1</sub>**, respectively.

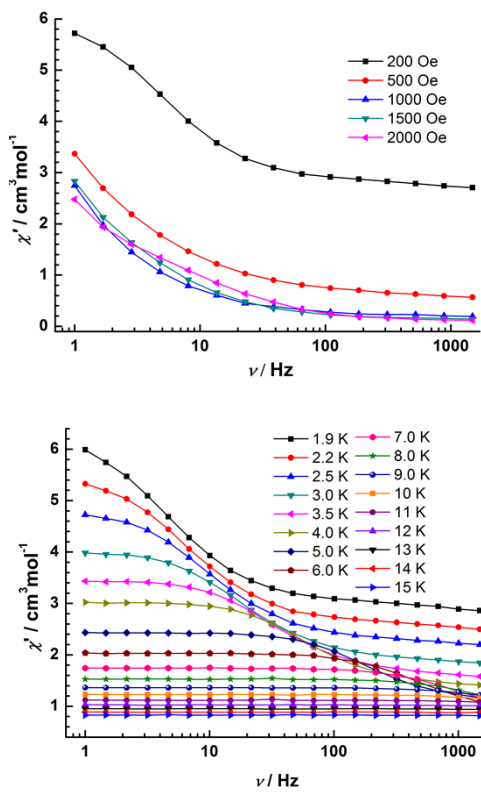


Fig. S7 Top: Frequency dependence of the in-phase ac susceptibility under various applied fields at 1.9 K for **R-Dy<sub>1</sub>**. Bottom: Frequency dependence of the in-phase ac susceptibility between 1.9 and 15 K at  $H_{\text{dc}} = 200$  Oe for **R-Dy<sub>1</sub>**. The solid lines are guides for the eyes.

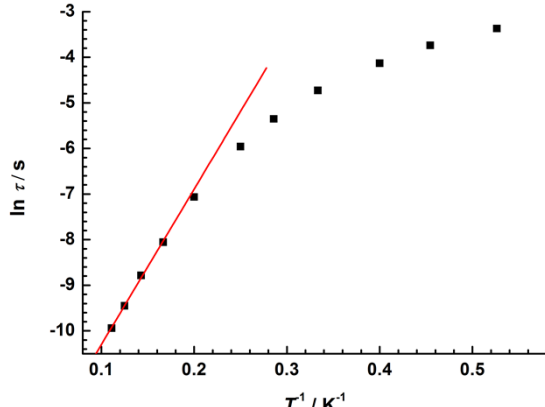


Fig. S8 Plot of relaxation time ( $\tau$ , natural logarithmic scale) vs. temperature (reciprocal scale) extracted from frequency-dependent data between 1.9 and 9.0 K, by fitting the  $\chi''$  vs. frequency curves for R-Dy<sub>1</sub>. The red line represents a linear fit to the Arrhenius equation, affording an effective energy barrier 34.5 K and pre-exponential factors ( $\tau_0$ ) of  $1.1 \times 10^{-6}$ .

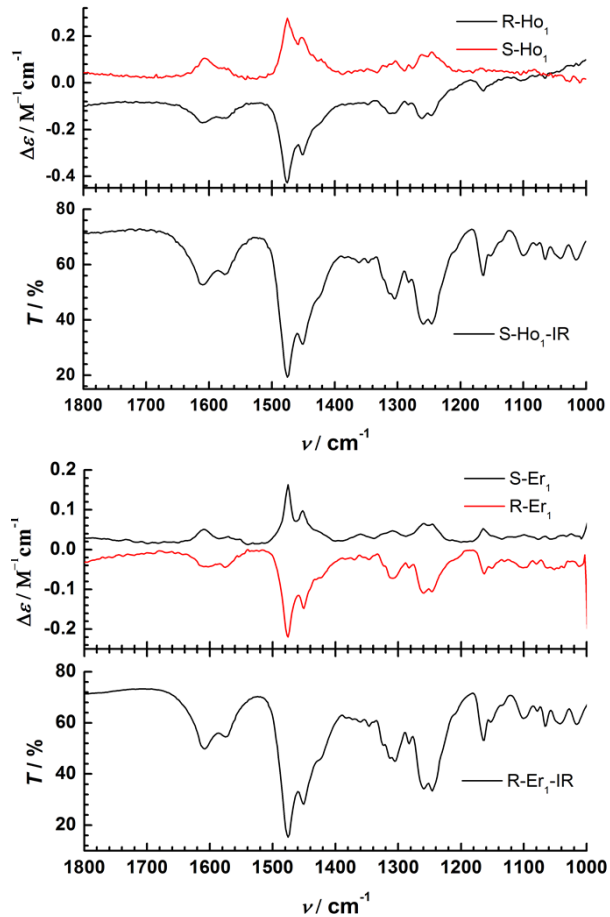


Fig. S9 Comparison of IR and VCD spectra observed for complexes R/S-Ho<sub>1</sub> and R/S-Er<sub>1</sub>.

**Table S1.** Bond lengths [ $\text{\AA}$ ] and angles [ $^{\circ}$ ] for R/S-Dy<sub>1</sub>, R/S-Ho<sub>1</sub> and R/S-Er<sub>1</sub>.

	R-Dy <sub>1</sub>	S-Dy <sub>1</sub>	R-Ho <sub>1</sub>	S-Ho <sub>1</sub>	R-Er <sub>1</sub>	S-Er <sub>1</sub>
Dy(1)-O(3)	2.194(10)	2.232(17)	2.186(12)	2.206(11)	2.135(14)	2.214(11)
Dy(1)-O(2)	2.202(7)	2.202(9)	2.215(7)	2.199(7)	2.219(8)	2.200(7)
Dy(1)-O(1)	2.239(10)	2.245(14)	2.211(10)	2.233(10)	2.210(12)	2.180(10)
Dy(1)-N(7)	2.406(10)	2.43(2)	2.384(12)	2.397(10)	2.388(12)	2.398(11)
Dy(1)-N(8)	2.446(9)	2.447(19)	2.436(11)	2.436(11)	2.403(15)	2.378(10)
Dy(1)-N(5)	2.520(8)	2.519(12)	2.500(8)	2.509(8)	2.533(11)	2.499(8)
Dy(1)-N(6)	2.531(8)	2.545(11)	2.540(8)	2.526(8)	2.498(9)	2.494(8)
O(3)-Dy(1)-O(2)	85.1(3)	85.0(5)	84.7(3)	85.1(3)	85.1(4)	84.5(3)
O(3)-Dy(1)-O(1)	170.1(4)	171.0(7)	169.7(4)	170.0(4)	169.2(4)	167.7(3)
O(2)-Dy(1)-O(1)	85.0(3)	86.3(5)	85.0(3)	84.9(3)	84.1(4)	83.2(3)
O(3)-Dy(1)-N(7)	84.7(4)	82.8(7)	83.7(4)	84.4(4)	94.8(5)	94.4(4)
O(2)-Dy(1)-N(7)	80.7(3)	80.7(5)	80.3(4)	81.1(3)	80.6(4)	79.1(3)
O(1)-Dy(1)-N(7)	93.9(4)	94.0(7)	94.2(4)	94.1(4)	83.9(5)	82.7(4)
O(3)-Dy(1)-N(8)	97.3(4)	99.1(7)	97.5(4)	97.8(4)	80.6(5)	81.3(4)
O(2)-Dy(1)-N(8)	81.9(3)	82.4(5)	82.0(3)	81.6(3)	81.9(4)	83.5(3)
O(1)-Dy(1)-N(8)	81.0(4)	81.6(6)	81.4(4)	80.8(4)	97.4(5)	98.0(4)
N(7)-Dy(1)-N(8)	162.3(3)	162.8(5)	162.0(3)	162.3(3)	162.2(4)	162.4(3)
O(3)-Dy(1)-N(5)	76.7(3)	77.2(5)	77.4(3)	76.7(3)	78.0(4)	78.5(3)
O(2)-Dy(1)-N(5)	146.8(3)	146.3(4)	147.1(3)	146.2(3)	146.3(3)	146.0(3)
O(1)-Dy(1)-N(5)	111.9(3)	111.4(5)	111.8(3)	112.0(3)	111.5(4)	111.7(3)
N(7)-Dy(1)-N(5)	124.1(3)	124.1(5)	124.2(4)	124.2(3)	72.1(4)	73.2(3)
N(8)-Dy(1)-N(5)	73.3(3)	72.7(5)	73.3(3)	73.1(3)	122.9(4)	122.0(3)
O(3)-Dy(1)-N(6)	111.0(3)	110.3(5)	111.2(3)	110.7(3)	111.3(4)	113.7(3)
O(2)-Dy(1)-N(6)	146.6(3)	146.8(4)	146.1(3)	146.4(3)	146.8(3)	146.7(3)
O(1)-Dy(1)-N(6)	77.8(3)	76.5(5)	77.6(3)	78.0(3)	78.0(4)	77.4(3)
N(7)-Dy(1)-N(6)	72.3(3)	72.6(5)	72.4(3)	71.7(3)	124.2(4)	124.1(3)
N(8)-Dy(1)-N(6)	122.5(3)	121.8(5)	123.0(3)	122.9(3)	73.1(4)	72.8(3)
N(5)-Dy(1)-N(6)	66.6(3)	66.9(4)	66.9(3)	67.3(3)	66.8(3)	67.2(3)

**Table S2.** The CShM values calculated by *SHAPE* 2.1 for seven-coordinated R/S-Dy<sub>1</sub>, R/S-Ho<sub>1</sub> and R/S-Er<sub>1</sub>.

	Pentagonal bipyramid	Capped octahedron	Capped trigonal prism
R-Dy1	4.433	2.016	0.795
S-Dy1	4.447	1.873	0.860
R-Ho1	4.421	2.046	0.813
S-Ho1	4.388	1.964	0.813
R-Er1	4.454	2.079	0.869
S-Er1	4.719	1.879	0.737

**Table S3.** Relaxation fitting parameters from Least-Squares Fitting of cole-cole plots.

T	$\chi_s$	$\chi_T$	$\alpha$
1.9	2.97024	6.42443	0.1934
2.2	2.65944	5.50294	0.12992
2.5	2.17142	4.95246	0.24911
3.0	1.81079	4.08256	0.21673
3.5	1.54611	3.48079	0.18625
4.0	1.36903	3.03768	0.14443
5.0	1.09253	2.43416	0.10562
6.0	0.88594	2.03334	0.11255
7.0	0.6845	1.74511	0.13715
8.0	0.38442	1.53316	0.20364